sciendo Applied Mathematics and Nonlinear Sciences, 9(1) (2024) 1-20

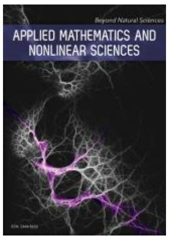

Applied Mathematics and Nonlinear Sciences

https://www.sciendo.com

Research on energy-saving strategies in the architectural design of the Eastern Railway in the era of artificial intelligence

Jianjun Xu[1,†]

1. Faculty of Civil and Architectural Engineering, Northeast Petroleum University, Daqing, Heilongjiang, 163318, China.

Submission Info

Communicated by Z. Sabir
Received December 11, 2023
Accepted December 18, 2023
Available online January 31, 2024

Abstract

This paper takes the air conditioning energy consumption in railroad building design as the main object of analysis and uses an orthogonal experimental design method to study the influencing factors and effects of energy consumption in the Middle East railroad construction design. Stochastic working condition simulation is carried out for the typical models of passenger stations in five climate zones to obtain the data set of the passenger station energy consumption model, and the multiple linear regression prediction models of air conditioning energy consumption in different regions are established. Combined with the hour-by-hour average outdoor temperature, hour-by-hour passenger flow and lighting and related equipment data in the waiting hall of a city in July, the air-conditioning cold load of railroad passenger stations is simulated and analyzed. Explore the implementation effect of energy-saving strategies for railroad passenger station air-conditioning system, and for the traditional PID control strategy, put forward the control strategy based on model prediction, analyze the change of centralized air-conditioning system cold load and the change of the actual performance coefficient of the chiller unit under different control strategies. The data show that compared with the traditional PID control, the model prediction control reduces the total energy consumption by 0.2063, which realizes the energy-saving optimization of the air conditioning system for railroad building design.

Keywords: Orthogonal experimental design; Conventional PID control; Multiple linear regression; Energy modeling; Railroad buildings.
AMS 2010 codes: 68T01

†Corresponding author.
Email address: 17745297826@163.com

ISSN 2444-8656
https://doi.org/10.2478/amns-2024-0022

1 Introduction

The concept of a low carbon economy has become increasingly significant in the development of the national economy, mainly through the form of low energy consumption, low pollution and low emissions to achieve a substantial reduction in carbon dioxide emissions so as to achieve the goal of the basic economic development model of low carbon economy.

With the construction of new and expanded railroads entering the peak period, the number of railroad buildings, specifically new railroad passenger stations, is gradually increasing [1-2]. The consumption of energy and resources continues to increase, and carbon dioxide emissions have risen dramatically, exerting great pressure on both the resource field and the environmental field and causing serious obstacles to the smooth development of the low-carbon economy [3-4].

Among them, the thermal insulation and heat preservation problem of railroad buildings is the main cause of energy loss [5]. It can be seen that a reasonable analysis of the energy-saving design technology methods of railroad buildings has certain practical significance for the smooth development of the concept of a low-carbon economy [6]. Usually, railroad buildings have the basic characteristics of diversity, specialization and independence, and it is very necessary to master the technical methods of energy-saving design of railroad buildings in order to realize the low-carbon development of railroad buildings [7-8]. Railroad building energy consumption in the railroad overall energy consumption in considerable proportions, so it is necessary to effectively control carbon dioxide emissions so as to achieve the basic energy-saving goals of low energy consumption and low pollution. The design of railroad building energy saving links needs to start from the point of view of railroad-building energy saving for the different climatic characteristics of the region, the building protection framework for improvement in order to achieve the purpose of improving the heat transfer resistance of the protection framework, reduce the amount of heat loss of the thermal insulation performance, and then ensure the rapid development of railroad buildings [9].

Huler, M. Et al. emphasized that no inspection methodology is universally valid and sustainable for ensuring code compliance. The study analyzes the specific requirements in the guidelines of Deutsche Bahn on the technical design of railroad construction structures and analyzes the feasibility of BPMN and DMN in the rules [10]. Qi, Q. Et al. Propose a green and energy-saving design method based on computer intelligence, aiming to solve the problem of the high structural weight of a certain type of crane with serious steel consumption. To achieve the goal of minimizing the crane structure's self-weight, two optimization models have been proposed. The results show that the main beam processing waste is reduced after fuzzy comprehensive optimization [11]. Yoshida, H. K. K. believes that the effective use of train renewable energy has a certain research value in the energy saving of electrified railroads, and thus proposes the reinforcement learning based on an actor-critic algorithm to realize the effective control of battery charging and discharging, which is able to autonomously learn the control strategies to achieve a stable balance between power supply and demand [12]. Akbari, S. Et al. study aimed to reduce the operating costs and carbon emissions of smart railway stations and their ancillary commercial buildings by designing and proposing an energy hub system, which consists of power, heating, and cooling sub-energy hubs. The study explores the impact of implementing DRP, utilizing recovered energy and adopting energy storage on operating costs and carbon emissions using fuzzy techniques for optimization purposes and incorporating seven case studies [13]. Li, Z. Et al. proposed a feed-forward air-conditioning temperature control method for high-speed railroad sleeper carriages in order to improve the energy efficiency of the train and combined it with the techniques of image recognition to detect the number and the type of passengers in each carriage, as well as verifying it through numerical simulation. Type, as well as verifying the effectiveness and feasibility of the proposed method through numerical simulation [14]. Jiang, L. Et al. proposed an integrated management system of electric-thermal energy for high-speed railroads, which mainly consists of two parts: the operation model of the electric-thermal integrated system and the coordinated control of the privacy and interests of the train dispatch centers and the stations by the alternate direction method based on the multiplier algorithm. A high-speed railroad analysis was conducted with six stations in North China to study its feasibility [15]. Thadani, H. L. Et al. designed an optimal vertical-axis wind turbine using the Malaysian high-speed railway as a research object. The results showed an average cost saving of RM16.7 million per year at the railway station, with a battery capacity of 12 hours per day. [16].

Tomita, M. Et al. showed that energy issues are of increasing concern, and in the case of railroad transportation, it is important to assess the situation in the railroad transportation sector. The study proposes a new railroad transmission feeder system using superconducting materials, and in order to validate the system, a superconducting feeder system was set up on a test track and operational tests were carried out. The energy data showed that the system can achieve energy savings under the average track model [17]. Miao, R. Et al. proposed a distance-based hybrid integer linear programming model that combines the NS position planning with the energy-efficient train control problem and optimizes the NS position and train speed trajectories. The main contribution of the study is that, for the proposed model, a number of case studies were conducted to explore the mechanism of train operation location on total energy consumption [18]. Tong, H. Et al. found that the current implementation of the road-to-rail policy was not well evaluated operationally due to the lack of real-world diesel locomotive emission measurements. Thus, the study conducted emission measurements of 245 active diesel locomotives on real railroad tracks to provide data for the evaluation of the environmental benefits of the implementation of the railroad alternative to long-distance highway policy [19].

Proposed a distance-based hybrid integer linear programming model that combines NS position planning with the energy-efficient train control problem and optimizes the NS position and train speed trajectory. Based on the energy consumption model analysis data set, five multiple linear regression prediction models for air conditioning energy consumption were established for each of the five climate zones: frigid, cold, hot summer and cold winter, hot summer and warm winter, and mild. The hour-by-hour average outdoor temperature of a city in July is taken as the basic data, and the static and dynamic load simulation results of air conditioning in passenger stations are discussed in the context of the hour-by-hour passenger flow of the railroad station and the power of the lighting and related equipment in the waiting hall. The energy-saving effect of the air-conditioning system in the railroad station is analyzed in terms of the energy-saving effect of the building envelope and the energy-saving measures of the air-conditioning system under natural ventilation. Aiming at the traditional PID control strategy, a model-based predictive control strategy is proposed to establish a simulation model of energy consumption in the waiting hall of the railroad station and analyze and verify the time-by-time simulation energy consumption of the centralized air conditioning system under different control strategies.

2 Method

2.1 Energy efficient technologies in the design of Middle East Railway buildings

With the development of the artificial intelligence era, railroads need to be built and expanded gradually. The consumption of energy and resources must be increased in this process, and carbon dioxide emissions will gradually increase. In the actual construction process, the demand for energy and resources will increase.

Combined with the summary of previous studies and the actual investigation of energy consumption in railroad building design, the correlation analysis of the number of stations using different energy-saving designs and technologies with the time of commissioning of the passenger station, the climate zone and the size of the station building using the SPSS software can obtain the energy-saving features of the Middle East railroad building design. That is, the energy-saving design started by focusing on “lighting system” and “heating, ventilation and air conditioning” and has developed different composite design paths. Currently, the overall design adopts the strategy of “passive priority, active optimization”, and the design simulation of air conditioning system zoning intelligent control, natural ventilation with heat pressure, and the use of openable glass curtain walls are widely used in non-cold regions. Therefore, this paper mainly analyzes and researches the energy consumption of air conditioning systems in railroad building design, aiming to improve the energy-saving effect of air conditioning systems.

2.2 Railway building air-conditioning energy consumption influencing factors

The air conditioning system is the main energy-consuming equipment in passenger stations, and to realize the energy saving of the air conditioning system, the first step is to find out the main factors affecting the energy consumption of the air conditioning system. Orthogonal experimental design can effectively reduce the number of tests and has high efficiency [20].

Analysis of variance (ANOVA) is mainly used to determine the primary and secondary order of factors through the significance test; the key lies in the decomposition of the sum of squares of the deviations. Suppose an orthogonal experiment has S factor, each factor takes m levels, and a total of i trials are done according to a certain scheme, then it can be considered that the difference between the experimental results is caused by two reasons. One is the fluctuation of the indicator value brought about by the level change of the factor, and the other is the fluctuation of the indicator value brought about by the experimental error.

1) The total sum of squared deviations:

$$S_r = \sum_{i=1}^{12}\left(y_i - \bar{y}\right)^2, \text{ of which } \bar{y} = \frac{1}{12}\sum_{i=1}^{12} y_i \tag{1}$$

Where S_T is the total sum of squared deviations, reflecting the total fluctuation of the experimental indicator values.

i is the number of experiments, $i = 1, 2, \cdots 12$.

y_i is the experimental results, the i th energy consumption value.

$\bar{y}$ for the average of the experimental results, that is, the average of the experimental results of the energy consumption value.

2) The sum of squared deviations of factors:

$$S_j = \frac{I_j^2 + II_j^2 \cdots}{M} - \frac{\left(\sum_{i=1}^{n} y_i\right)^2}{X} \tag{2}$$

Where S_j is the sum of squared deviations of the factors, reflecting fluctuations in the indicator values due to changes in the level of the j nd factor.

j is the different factors affecting energy consumption, $j = 1, 2, \cdots 10$.

I_j is the value of energy consumption for factor j with coefficient level 1.

II_j is the value of energy consumption for factor level 2 of factor j.

M is the number of replications of factor levels in orthogonal experiments, $M = 6$.

X is the total number of orthogonal experiments, $X = 12$.

3) Error sum of squares

The difference between the total sum of squared deviations and the sum of squared deviations of the factors is the sum of squared errors S_e, i.e.:

$$Se = S_{T^-}\left(S_1 + S_2 + \cdots + S_{10}\right) \tag{3}$$

4) Degrees of freedom

The degrees of freedom for each sum of squared deviations are:

$$f_T = X - 1 \tag{4}$$

$$f_j = M - 1 \tag{5}$$

$$f_e = f_T - \sum_{j=1}^{s} f_j \tag{6}$$

Where f_T is the degrees of freedom of the total deviation.

f_j is the degrees of freedom of factor deviation.

f_e is the degree of freedom of the error.

5) F-distribution ordering

It can be proved that the sum of squares of the above deviations obey the distribution of x^2, so we can construct the statistic F_j according to the distribution characteristics of x^2 and the distribution of j factors obey the distribution of x^2. According to the difference of statistic F_j, we can sort out the primary and secondary relationship between the factors:

$$\overline{S_e} = S_e / f_e \tag{7}$$

$$\overline{S}_j = S_j / f_j \tag{8}$$

$$F_j = \overline{S}_j / \overline{S}_e \tag{9}$$

Where $\overline{S}_e$ is the error mean square value.

$\overline{S}_j$ is the factor mean square value.

F_j is the statistic of j factors obeying x^2 distribution.

2.3 Railway building energy consumption prediction model

2.3.1 Energy modeling analysis data sets

The energy consumption composition of the railroad passenger station building is more complicated, with numerous connections and determining factors. In order to calculate the weight of each influencing factor, as well as by determining the influencing factors to get the final building energy consumption results, 10 parameters are selected as the object of study, and 3 different input values are selected for each parameter, and the specific data are shown in Table 1. It is possible to produce 312 simulation results, randomly selected 300 groups of working conditions, each climate zone is simulated separately, and 5 sets of data are obtained, which are used as the data set for analyzing the energy consumption model of the passenger terminal.

Table 1. Main design parameters that affect energy consumption

Parameter	Different input values		
	1	2	3
Boiler efficiency BE	89	95	100
Boiler cold water setcop	4.9	5.5	5.7
Summer setting temperature SST	26	29	30
Winter setting temperature WST	19	22	25
Osmotic wind PA	0.8	1.1	1.2
Window ratiowwr	0.6	0.7	0.9
Thermal coefficient of sun SGHC	0.4	0.5	0.6
Maximum aggregate MP	6500	8000	9500
Lighting power densitylq	9	11	13
Equipment power densityeq	12	17	23

In the actual situation, the operation mode of the unit is turned on throughout the year, and the air conditioner is turned on when the indoor temperature is higher than the set temperature in the above table in the summer operation time, and the natural ventilation is turned on at night, and the set temperature at 22:00~05:00 at night is 30℃. In winter, heating is turned on when it is lower than the set temperature, and the set temperature at 05:00~22:00 is selected according to the above table, and the set temperature at 22:00~05:00 the next day is 12℃. Other fixed parameters are shown in Table

2. The solar heat gain coefficient for the cold region is fixed at 0.82, and the heat transfer coefficients of the exterior walls and windows are 0.418 $W/(m^2 \cdot k)$ and 1.85 $W/(m^2 \cdot k)$ respectively.

Table 2. Other parameter Settings in various climatic areas

Parameter	Cold	Cold	Summer heat	Summer heat	Mildness
Roof heat transfer coefficient	0.38	0.39	0.37	0.503	0.498
External wall heat transfer coefficient	0.418	0.418	0.55	0.799	0.802
Outer window heat transfer coefficient	1.85	1.95	2.34	2.67	2.68
The heat transfer coefficient of the roof	1.81	1.85	2.36	2.59	2.64

2.3.2 Air-conditioning energy consumption prediction regression model

1) Cold region

The combined expression of the heating and air conditioning energy consumption prediction regression model Y_1 and the total energy consumption prediction regression model Y_1' for the passenger stations in this region is equation (10):

$$\begin{cases} Y_1 = \beta_0 + \beta_1 WWR + \beta_2 SST + \beta_3 WST + \beta_4 MP + \beta_5 LQ + \beta_6 EQ \\ \qquad + \beta_7 PA + \beta_8 COP + \beta_9 BE \\ Y_1' = \beta_0 + \beta_1 WWR + \beta_2 SST + \beta_3 WST + \beta_4 MP + \beta_5 LQ + \beta_6 EQ \\ \qquad + \beta_7 PA + \beta_8 COP + \beta_9 BE \end{cases} \tag{10}$$

The multiple regression coefficients of the energy consumption prediction model are shown in Table 3. In the severe cold region, for heating and air conditioning energy consumption Y_1 and total energy consumption Y_1', the coefficients of the constant term and the first four variables of the regression model are the same, which are 309.25, 24.88, 6.98, 10.05, and 0.003, respectively.

Table 3. The multivariate regression coefficient of energy prediction model

	β_0	β_1	β_2	β_3	β_4	β_5	β_6	β_7	β_8	β_9
Y_1	309.25	24.88	-6.98	10.05	0.003	-0.18	-0.89	111.23	-5.64	-2.14
Y_1'	309.25	24.88	-6.98	10.05	0.003	4.52	5.56	111.23	-5.64	-2.14

2) Cold regions

The combined expression of the heating and air conditioning energy consumption prediction regression model Y_2 and the total energy consumption prediction regression model Y_2' for the passenger terminal in this region is equation (11):

$$\begin{cases} Y_2 = \beta_0 + \beta_1 WWR + \beta_2 SST + \beta_3 WST + \beta_4 SGHC + \beta_5 MP + \beta_6 LQ \\ \qquad + \beta_7 EQ + \beta_8 PA + \beta_9 COP + \beta_{10} BE \\ Y_2' = \beta_0 + \beta_1 WWR + \beta_2 SST + \beta_3 WST + \beta_4 SGHC + \beta_5 MP + \beta_6 LQ \\ \qquad + \beta_7 EQ + \beta_8 PA + \beta_9 COP + \beta_{10} BE \end{cases} \tag{11}$$

The multiple regression coefficients of the energy consumption prediction model are shown in Table 4. From the regression coefficients in the table, it can be seen that unlike the severe cold region, there is a large difference between the coefficients of Y_2 and Y_2' in WWR, with the former being 8.14, and the latter being significantly smaller than the former, achieving only 5.82.

Table 4. The multivariate regression coefficient of energy prediction model

	β_0	β_1	β_2	β_3	β_4	β_5	β_6	β_7	β_8	β_9	β_{10}
Y_2	167.96	8.14	-6.55	7.23	55.89	0.004	0.14	-0.31	69.58	-4.96	-0.85
Y_2'	189.24	-5.82	-7.92	6.85	69.36	0.005	4.76	5.78	69.77	-4.63	-0.66

3) Hot summer and cold winter areas

The combined expression of the heating and air conditioning energy consumption prediction regression model Y_3 and the total energy consumption prediction regression model Y_3' for the passenger terminal in this region is equation (12):

$$\begin{cases} Y_3 = \beta_0 + \beta_1 WWR + \beta_2 SST + \beta_3 WST + \beta_4 SGHC + \beta_5 MP + \beta_6 LQ \\ \qquad + \beta_7 EQ + \beta_8 PA + \beta_9 COP + \beta_{10} BE \\ Y_3' = \beta_0 + \beta_1 WWR + \beta_2 SST + \beta_3 WST + \beta_4 SGHC + \beta_5 MP + \beta_6 LQ \\ \qquad + \beta_7 EQ + \beta_8 PA + \beta_9 COP + \beta_{10} BE \end{cases} \tag{12}$$

The multiple regression coefficients of the energy consumption prediction model are shown in Table 5. The air-conditioning energy consumption and total energy consumption in the hot summer and cold winter regions also agree with the cold regions on variable WWR, and the coefficients satisfy $\beta_1 = 12.3$.

Table 5. The multivariate regression coefficient of energy prediction model

	β_0	β_1	β_2	β_3	β_4	β_5	β_6	β_7	β_8	β_9	β_{10}
Y_3	200.51	12.3	-8.66	5.09	77.56	0.0028	0.28	0.39	36.58	-6.99	-0.36
Y_3'	200.55	12.3	-8.66	5.09	77.56	0.0028	4.97	6.53	36.58	-6.99	-0.36

4) Hot summer and warm winter areas

The combined expression of the heating and air conditioning energy consumption prediction regression model Y_4 and the total energy consumption prediction regression model Y_4' for the passenger terminal in this region is equation (13):

$$\begin{cases} Y_4 = \beta_0 + \beta_1 WWR + \beta_2 SST + \beta_3 SGHC + \beta_4 MP + \beta_5 LQ + \beta_6 EQ \\ \qquad + \beta_7 PA + \beta_8 COP \\ Y_4' = \beta_0 + \beta_1 WWR + \beta_2 SST + \beta_3 SGHC + \beta_4 MP + \beta_5 LQ + \beta_6 EQ \\ \qquad + \beta_7 PA + \beta_8 COP \end{cases} \tag{13}$$

The multiple regression coefficients of the energy consumption prediction model are shown in Table 6. Except for β_5 and β_6, the coefficients of the remaining terms differ very little, and even the coefficient at variable MP achieves 0.005.

Table 6. The multivariate regression coefficient of energy prediction model

	β_0	β_1	β_2	β_3	β_4	β_5	β_6	β_7	β_8
Y_4	313.63	17.42	-10.33	113.75	0.005	0.86	1.53	9.86	-10.67
Y_4'	313.58	18.43	-10.65	114.25	0.005	5.63	7.68	11.03	-9.49

5) Moderate region

The combined expression of the heating and air conditioning energy consumption prediction regression model Y_5 and the total energy consumption prediction regression model Y_5' for the passenger terminal in this region is equation (14):

$$\begin{cases} Y_5 = \beta_0 + \beta_1 WWR + \beta_2 SST + \beta_3 WST + \beta_4 SGHC + \beta_5 MP + \beta_6 LQ \\ \qquad + \beta_7 EQ + \beta_8 PA + \beta_9 COP + \beta_{10} BE \\ Y_5' = \beta_0 + \beta_1 WWR + \beta_2 SST + \beta_3 WST + \beta_4 SGHC + \beta_5 MP + \beta_6 LQ \\ \qquad + \beta_7 EQ + \beta_8 PA + \beta_9 COP + \beta_{10} BE \end{cases} \tag{14}$$

The multiple regression coefficients of the energy consumption prediction model are shown in Table 7. There is a significant difference between air conditioning energy consumption Y_5 and total energy consumption Y_5' in moderate areas only at LQ, EQ two variables, and the regression model has 100% synchronization on the constant term and the rest of the variables.

Table 7. The multivariate regression coefficient of energy prediction model

	β_0	β_1	β_2	β_3	β_4	β_5	β_6	β_7	β_8	β_9	β_{10}
Y_5	101.89	16.78	-5.57	3.04	92.55	0.005	0.34	0.36	9.77	-3.78	-0.18
Y_5'	101.89	16.78	-5.57	3.04	92.55	0.005	5.12	6.65	9.77	-3.78	-0.18

3 Result and discussion

3.1 Simulation of energy-consuming building cooling loads in Middle East Railway passenger stations

With the continuous development of intelligent buildings, the air conditioning load is occupying a considerable proportion of the building's energy consumption. Reducing the energy consumption of air conditioning systems and creating green, energy-efficient buildings have become the goals to pursue in the era of artificial intelligence. For the public building of the railway station that has been put into use, how to scientifically and accurately simulate the amount of cold load of the railway station building during operation so as to effectively and reasonably control the operation of the air conditioning system is the key to reducing the energy consumption of this building.

Before conducting the cold load simulation, it is necessary to collect relevant equipment parameters, outdoor air parameters, and hourly passenger flow to prepare accordingly. The following cold load simulation parameters are partly obtained through on-site record checking and partly referred to the relevant values in the "Design Code for Railway Passenger Stations" as an aid.

1) July outdoor hourly average temperature of a city

The hour-by-hour fresh air load is determined by the minimum fresh air volume and the hour-by-hour outdoor air enthalpy, and the meteorological-specific data are shown in Table 8. During the 8:00-13:00 time span, the temperature of the city's wet bulbs is higher than 27°C, and it reaches a maximum of 27.59°C at 9:00 p.m. The enthalpy value stays within the range of 77 to 89 throughout the day.

Table 8. Meteorological data

Time	8:00	9:00	10:00	11:00	12:00
Wet bulb temperature	27.56	27.59	27.45	27.53	27.32
Hour enthalpy	89.42	89.62	89.41	88.05	87.72
Time	13:00	14:00	15:00	16:00	17:00
Wet bulb temperature	27.03	26.75	26.33	26.01	25.62
Hour enthalpy	86.45	84.92	89.33	88.05	80.32
Time	18:00	19:00	20:00	21:00	22:00
Wet bulb temperature	25.42	25.19	25.06	25.05	25.09
Hour enthalpy	79.23	78.24	77.68	77.38	77.48

2) Hourly passenger flow

The dynamic load simulation calculation will use hour-by-hour passenger flow prediction as the basic data, and the data format is the total number of people in the waiting hall per hour in a specific period. Table 9 displays the daily passenger flow target. 21:00-22:00 hours, the passenger flow is less. It is 889 at 22:00 and reaches the lowest value during the day.

Table 9. Target day traffic distribution

Time	8:00	9:00	10:00	11:00	12:00
Passenger flow	2775	3568	4028	4421	4648
Time	13:00	14:00	15:00	16:00	17:00
Passenger flow	4149	4775	5204	4998	5268
Time	18:00	19:00	20:00	21:00	22:00
Passenger flow	5789	5679	5508	1039	889

3) Lighting and related equipments in waiting halls

According to the relevant information and research, the effective area of the waiting hall and entrance hall of the train station is 107,562.3 m^2, and the related equipment statistics are shown in Table 10. The railroad waiting hall includes 10 sets of security equipment, and each security equipment set has a power of 800 W. There are 18 vertical elevators and 25 escalators, each with a power of 9300 W and 8400 W. The number of railroad waiting halls is 10, and each security equipment has a power of 800 W. The number of the railroad waiting halls is 10, and the power of each security equipment is 800 W.

Table 10. Equipment information statistics

Serial number	Device name	Power	Quantity
1	Security equipment	800W	The 10 sets
2	Vertical elevator	9300W	The 18 sets
3	Escalator	8400W	The 25 sets
4	Shop	7000W	The 25 sets
5	Advertising light box	Large780W Small 450W	A total of 46
6	Emergency evacuation sign	1.5W	About 550
7	Emergency evacuation indicator	3.6W	About 640
8	Automatic ticket check-in machine	630W	Twenty-four sets
9	Automatic entry/exit brake machine	580W	Twenty-six sets

3.1.1 Static load simulation

Since this paper aims to focus on the Analysis of optimizing the cold distribution for some periods, it is only necessary to take the simulated values of the enclosure cold load for the period 8:00-23:00. The simulated values of cold load are shown in Table 11. The load values reach the maximum range at 16:00, 17:00 and 18:00 with a maximum value of 897.69.

Table 11. Cold load simulation value

Time	8:00	9:00	10:00	11:00	12:00
Load value	180.25	178.36	192.65	256.91	335.62
Time	13:00	14:00	15:00	16:00	17:00
Load value	425.36	593.68	811.20	897.69	889.12
Time	18:00	19:00	20:00	21:00	22:00
Load value	822.1	738.65	645.74	540.22	454.01

3.1.2 Dynamic load simulation

1) Personnel load calculation

For public buildings with large passenger flows, the main factors affecting the change of cold load are passenger flow and fresh air load. For large-scale railroad passenger terminals, the average daily number of passengers is more than 10,000, and they operate 24-hours. Because the functional division of the railroad passenger station building is relatively weak, and the mobility of people is relatively single, so in the calculation of the passenger flow prediction results directly as the total number of people entering the station hall and waiting hall. The cold load of the train station is calculated using the passenger flow load formula after knowing the hourly passenger flow distribution. The hour-by-hour cold load of the target daily passenger flow is shown in Table 12. Between 11:00 and 20:00, the main load of the train station is concentrated, yielding a total load value of 10730.75 KW.

Table 12. Target day passenger flow time cooling load

Time	8:00	9:00	10:00	11:00	12:00
Load(KW)	478.96	613.24	692.14	758.52	798.22
Time	13:00	14:00	15:00	16:00	17:00
Load(KW)	714.20	818.23	895.43	858.97	906.01
Time	18:00	19:00	20:00	21:00	22:00
Load(KW)	943.78	975.67	946.23	178.02	153.13

2) Calculation of fresh air load

The hourly fresh air load is determined by the minimum fresh air volume and the hourly enthalpy of indoor and outdoor air; refer to Table 8 for the hourly enthalpy and temperature of outdoor air in July in the specific city.

For indoor air's enthalpy, the dry bulb temperature is 28°C, and the relative humidity is 60%. Through the enthalpy and humidity diagram calculation software, the indoor enthalpy value is 65.63 KJ / kg, and according to the formula of fresh air load calculation, the hourly fresh air volume and fresh air load are shown in Table 13. The fresh air volume is 73771 at 19:00, and the value of the fresh air load is 308.45. The fresh air volume varies with changes in temperature, and an increase in fresh air volume represents an increase in fresh air load.

Table 13. New wind load

Time	8:00	9:00	10:00	11:00	12:00
Fresh air (m^3)	36065	46289	52391	57412	60342
Load(KW)	274.65	355.01	398.12	425.12	427.03
Time	13:00	14:00	15:00	16:00	17:00
Fresh air (m^3)	53912	61944	67600	64932	68452
Load(KW)	382.52	381.27	379.65	329.04	315.47
Time	18:00	19:00	20:00	21:00	22:00
Fresh air (m^3)	71335	73771	71538	13456	11493
Load(KW)	299.53	308.45	264.13	48.69	42.78

3.2 Analysis of the effect of energy-saving strategies in railroad station building design

3.2.1 Analysis of the energy-saving effect of building envelopes

1) Glass curtain wall

Several energy-saving glass materials are listed and simulated with the equest energy consumption simulation software for the waiting hall of the train station, and the simulation results are shown in Table 14. The shading coefficient of ordinary transparent glass is 0.96, and the heat transfer coefficient is 6.17 m^2, while the shading coefficient of coated insulating glass can reach 0.46, the shading coefficient is reduced by 0.5, and the visible light transmission rate is reduced by 0.42.

Table 14. Glass parameter statistics

Glass type	Heat transfer coefficient ($w/m2.K$)	Shade coefficient	Visible light transmittance
Ordinary hollow glass	3.21	0.84	0.64
Plain transparent glass (1001)	6.17	0.96	0.89
Low radiation glass (2631)	1.9	0.68	0.75
Coated hollow glass (2636)	2.51	0.46	0.47
Hot reflective glass (2406)	2.96	0.28	0.19

The data on the energy consumption of each building with different glass types is shown in Table 15. The data of different glass types in each building of the railroad yielded the highest total building energy consumption of 8669904kwh for ordinary glass, of which 4761105kwh or 0.5492 is for cooling energy, followed by 2538005kwh or 0.2927 for lighting energy.

Table 15. Different types of glass types of energy consumption data

	Basic building	Plain glass	Thermal reflector glass	Coated hollow glass	Low radiation glass
Refrigeration energy	4733768	4761105	3592821	4028635	4582156
Heating energy	728994	994245	1031235	892356	705723
Lighting energy	2581003	2538005	3062004	2681000	2573004
Equipment energy	376589	376589	376589	376589	376589
Architecture	8419778	8669904	8062478	7977325	8237541

2) Skylight size

As can be seen from the load composition of the air conditioning system in the previous section, the skylight occupies a considerable proportion of the peak cooling and heating load of the whole building. The peak cooling and heating loads of buildings with different skylight area ratios are shown in Table 16. The building's peak heat load is gradually increasing due to the increase in skylight area. Taking ordinary insulating glass as an example, at 5% skylight area ratio, the cold load is 7845, and the heat load is 2586. At a 35% skylight area ratio, the cold and heat loads are 11,268 and 3,576, respectively. The cold loads have gone up by 1.44 times.

Table 16. Different skylight area ratio of the building peak heat load

		Ordinary hollow glass	Plain glass	Low radiation glass	Coated hollow glass	Thermal reflector glass
5%	Cold load	7845	7890	7561	7306	7160
	Heat load	2586	3453	2336	2561	2819
10%	Cold load	8104	8245	7795	7536	7185
	Heat load	2906	3578	2365	2672	2879
15%	Cold load	8492	8775	8125	7871	7415
	Heat load	2968	3739	2399	2745	2974
20%	Cold load	9142	9508	8685	8297	7736
	Heat load	3095	3977	2445	2886	3135
25%	Cold load	9937	10205	9337	8814	8116
	Heat load	3245	4146	2526	3010	3298
30%	Cold load	10554	10957	10034	9456	8579
	Heat load	3396	4585	2607	3159	3517
35%	Cold load	11268	12575	10680	10085	9081
	Heat load	3576	4895	2689	3356	3745

3.2.2 Energy efficiency analysis of air-conditioning systems

1) Research on energy conservation in large temperature difference systems

The large temperature difference referred to is the temperature of the air conditioning air supply or water supply is greater than the temperature difference used in conventional air conditioning systems, and it is obvious that the large temperature difference between air conditioning systems is relative to the conventional air conditioning system. Due to the introduction of a significant difference in temperature during circulation, the flow of circulation will decrease, which can lead to a reduction in delivery energy consumption. Since the air conditioning system in the train station is a ground source heat pump system, it is appropriate to use a large flow rate and small temperature difference for the cooling water system, so the large temperature difference of the water system is only used for the chilled water system.

The energy saving effect of the chilled water system is analyzed to obtain the energy consumption of the air conditioning system with a large temperature difference, which is divided into three situations: basic building, large temperature difference without frequency conversion and large temperature difference with frequency conversion. The energy consumption of chilled water pumps is significantly reduced after the adoption of large temperature difference, especially the pumps in the adoption of frequency conversion after the energy saving effect of chilled water pumps is more significant, their energy saving rate of 16.5%, 54.2% respectively.

2) Energy saving Analysis of ventilation

To improve the indoor thermal environment and save air-conditioning energy, ventilation is a common technical measure in today’s buildings. Ventilation of buildings not only provides fresh air but also reduces indoor temperatures during the transitional season.

To analyze the effect of natural ventilation on the building during the transition season, a simulation of the waiting room was carried out using Equest. The air conditioner was turned off, and the ventilation times were set to 0.5 times/h, 1.5 times/h and 2 times/h, respectively, and the indoor temperatures in April, May, September and October were counted in the simulation with different numbers of natural ventilation times, as shown in Table 17.

In June, July and August, the number of ventilation increases, but the temperature inside the hall increases, so it is not energy-efficient to carry out natural ventilation in the most waiting hall in summer. In April, May, September and October, with the increase in the number of natural ventilation, the number of hours less than 26 degrees inside the waiting hall gradually increases, the number of hours between 26 and 32 degrees is decreasing, and the number of hours greater than 32 degrees is also gradually decreasing. In April, when the number of ventilation times is set to 2 times, the number of hours less than 26 degrees inside the hall is increased from 568 to 638 hours. The number of hours greater than 32 degrees also decreased by 3. After changing the ventilation frequency to 2 in October, there were only 5 hours in the hall that were higher than 26 degrees. Since 32 degrees is the maximum comfortable temperature range under natural ventilation, the air-conditioning can be turned off completely in April and October if it is well-ventilated. In May and September, after the ventilation frequency was increased to two times, the number of hours that were greater than 26 degrees was significantly reduced, and so the air-conditioning would be turned on less frequently.

Table 17. Natural ventilation affects the temperature of the cooling season.

	Ventilation 0.5 times			Ventilation 1 times			Ventilation 2 times		
	<26	26~32	>32	<26	26~32	>32	<26	26~32	>32
April	568	135	26	617	79	27	638	34	23
May	315	256	178	412	158	174	468	115	167
June	45	305	375	145	214	367	225	124	368
July	67	278	405	174	176	398	226	124	397
August	123	374	256	245	241	248	375	133	246
September	392	213	117	493	116	117	537	76	112
October	698	49	0	746	12	1	745	5	0

3.3 Simulation analysis of energy consumption of centralized air-conditioning system in railroad stations

Based on the simulation calculation of the air-conditioning cold load of the railroad passenger station in the previous section, a model predictive controller for the air-conditioning system is designed, and this section aims to demonstrate the control effect of the model predictive control on the air-conditioning system of the railroad passenger station through simulation experiments.

3.3.1 Establishment of Simulation Model of Energy Consumption in Waiting Halls of Railway Passenger Stations

The building energy consumption simulation model is set up in TRNSYS18/trnbuild, which contains commonly used wall and window databases and fully considers the effects of cold air infiltration, ventilation and indoor heat sources on the time-by-time energy consumption of the building. The construction of a multi-region building model can be realized simply by inputting the basic building information such as the length, width, height, envelope parameters, and the working condition of air-conditioning equipment of each region.

The external wall area of the air-conditioned area of the waiting hall is 425*2+1198*2 m^2, and the external wall area of the non-air-conditioned area is 478*2+1335*2 m^2. The roof area is 17385 m^2 , and the air coupling quantity is 36738kg/h. The heat dissipation of the personnel in the internal heat source accounts for 0.67 of heat radiation and 0.33 of heat convection, while the heat dissipation of equipment and lighting accounts for 0.60 of heat radiation and 0.40 of heat convection, and the humidity dissipation quantity is only considered to be dissipated by the personnel, and the size of which is set to 0.024 g/(h·m^2). The validity of the model can be verified after the parameters are determined.

June 1st to September 30th was selected as the simulation period. The presence of indoor heat sources, including personnel, equipment, and lighting, heat dissipation, makes it desirable that indoor temperatures should be higher than outdoor temperatures when uncooled. Moreover, the temperature in the unconditioned zone will be significantly higher than the temperature in the ground floor space, which is the conditioned zone is subject to higher solar radiation and poor heat dissipation due to the limited height and space of the roof insulation. It is easy to see that the results of the qualitative analysis are consistent with the simulation results obtained by TRNSYS, indicating that the building model in trnbuild can basically reflect the temperature changes in the waiting hall, and the model building is more accurate.

3.3.2 Time-by-time simulation analysis of energy consumption of centralized air-conditioning system under different control strategies

Based on the building model obtained in trnbuild in the previous section, a complete simulation model of the energy consumption of the centralized air conditioning system can be built in TRNSYS18/Simulation Studio. At the same time, the control strategy obtained in MATLAB can be applied to the simulation model of the air conditioning system built in TRNSYS. The simulation time is selected as the cooling season, i.e., from June 1st to September 30th. The simulated working time of the centralized air-conditioning system in the railroad passenger station is 2910 h. Its indoor environment and the energy consumption of the centralized air-conditioning system can be calculated by TRNSYS studio to obtain the time-by-time change of its indoor environment and centralized air-conditioning system. Subsequently, joint simulation will be carried out based on the model to prove the control and energy-saving effect of the model predictive control strategy.

1) Comparison of indoor environment comfort control effect

The time-to-time changes in indoor temperature and relative humidity in the waiting hall are obtained through TRNSYS studio simulation. The difference between the median indoor temperature and humidity under model predictive control and traditional PID control is relatively small. However, the upper and lower quartiles of temperature and humidity and the upper and lower boundaries of the spacing under PID control are significantly larger than that under model predictive control, which indicates that compared with the traditional PID control, the model predictive control can ensure that the indoor environment is maintained in the reasonable range near the target value. The fluctuation amplitude is small, which effectively avoids the phenomenon of overcooling and overheating.

2) Comparison of energy-saving effect of centralized air-conditioning system

The cold load change of the centralized air conditioning system under different control strategies is shown in Figure 1. The maximum value of the cold load of the air conditioning system under the traditional PID control strategy reaches 6500 KW, while under the MPC control strategy, the fluctuation amplitude of the cold load value of the air conditioning control system is small, and the maximum value does not exceed 6000 KW. It can be clearly seen from the simulation results that the centralized air conditioning system cold load fluctuates a lot under the traditional PID control strategy, and it is not possible to avoid the phenomenon of energy waste caused by poor matching of the loads when there is a large fluctuation in the change of outdoor temperatures. The energy waste phenomenon caused by inactive matching cannot be avoided even when the outdoor temperature fluctuates greatly. The cold load of the centralized air-conditioning system under model predictive control is significantly reduced compared with the traditional PID control strategy, and the fluctuation amplitude is relatively small.

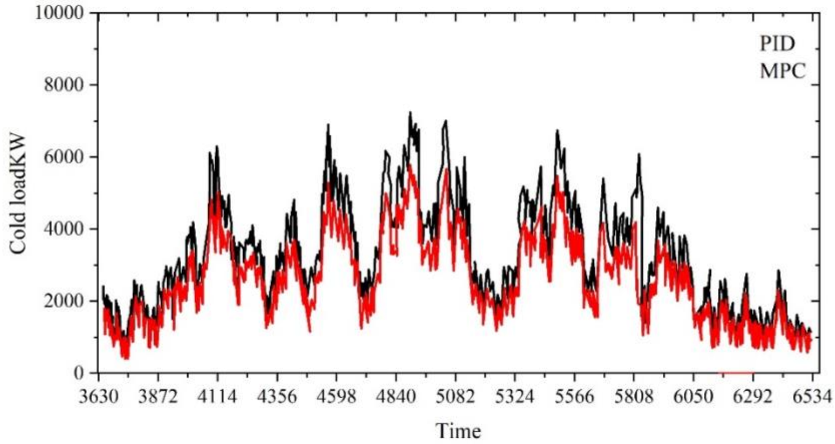

Figure 1. Cooling load of refrigerating monsoon car hall is changed by time

In addition, the chiller plant coefficient of performance (COP) is introduced to measure the efficiency of energy conversion during the operation of centralized air-conditioning systems. In general, when the cooling demand is equal, the higher the energy efficiency ratio, the lower the electricity consumption consumed by the air-conditioning unit.

The variation of the actual coefficient of performance of chiller units under different control strategies is shown in Figure 2. Under the traditional PID control strategy, the energy efficiency ratio of the air-conditioning chiller unit fluctuates greatly, and the fluctuation is the largest before and after the value of 4840. Under the MPC control strategy, the energy efficiency ratio of the group varies smoothly from time to time, and the energy efficiency is always maintained in the range of 3~4COP. From the simulation results, it can be seen that the energy efficiency ratio of the chiller unit under the model predictive control is relatively stable and can be maintained at a high level throughout the cooling season. The chiller efficiency ratio decreases significantly under the traditional PID control strategy when the temperature difference is large, or there is interference.

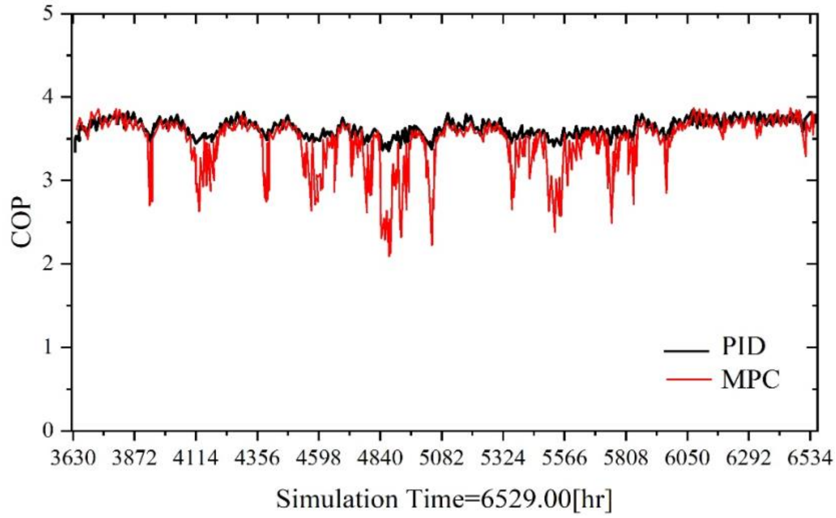

Figure 2. Different control strategies for cooling cold water units

Finally, the energy consumption of the centralized air conditioning system in the cooling season is calculated. Taking the total energy consumption of the centralized air conditioning system without control as a benchmark, the energy consumption of the centralized air conditioning system in the cooling season under different control strategies was counted to quantitatively explore the energy-saving efficiency of the centralized air conditioning system under the two control strategies, and the statistical results can be shown in Table 18.

The total energy consumption under the traditional PID control strategy is 393,136.0kwh, realizing an energy-saving efficiency of 0.1968. Compared to traditional PID control, the model predictive control reduces total energy consumption by 0.2063 when used with the traditional PID control strategy. The simulation results proved that the model predictive control energy saving efficiency is better than the traditional PID control, which is more in line with the demand for air conditioning control in railroad passenger stations.

Table 18. Cooling seasonal energy consumption statistics

	Energy consumption of cold water set kwh	Water consumption	Cooling tower energy consumption
Uncontrolled	427185.6	37887.2	9798.5
PID	341168.5	31632.9	7970.4
MPC	247936.1	26338.4	7128.2
	Energy consumption of the air processor group	Total energy consumption	Energy efficiency
Uncontrolled	14587.5	489458.8	0%
PID	12364.2	393136.0	19.68%
MPC	10754.9	292157.6	40.31%

4 Conclusion

This paper proposes a regression model for predicting the energy consumption of air conditioning in Middle East railway buildings, taking into account the main factors that affect energy consumption. Combined with the simulation results of the air-conditioning cold load in the Middle East Railway passenger station, it analyzes the implementation effect of energy-saving strategies for the air-conditioning system of the railroad passenger station in terms of the building envelope and the air-conditioning system. The design and proposal of a predictive controller model for the air conditioning system have been reviewed, and the energy-saving effect of the predictive control model has been analyzed and verified.

Based on the cold load simulation results of the energy consumption of Middle East Railway passenger station buildings, the effect of the energy-saving strategy of railroad passenger station building design is examined. The maximum value of the cold load of the air conditioning system under the traditional PID control strategy reaches 6500 KW, while the maximum value of the cold load of the air conditioning system under the MPC control strategy does not exceed 6000 KW, and the fluctuation of the value of the cold load is small. An energy-saving efficiency of 0.1968 can be realized under the traditional PID control strategy, while the MPC model predictive control proposed in this paper reduces the total energy consumption by 40.31%. The simulation results prove that the model predictive control energy-saving efficiency is better than the traditional PID control, which is more in line with the demand of air conditioning control in railroad passenger stations.

The purpose of this paper is to propose a model-based predictive controller for the PID control strategy commonly used at this stage, and simulation verification is carried out. The simulation experiment proves that the predictive control model not only achieves better control effects, but also achieves the goal of reducing energy consumption of centralized air-conditioning systems. It provides a new direction for the energy-saving technology in the Middle East Railway building design.

References

[1] Zhou, X., Lin, X., Ji, X., & Liang, J. (2021). Effects of high-speed railway construction and operation on related industries in china. Sustainability, 13.

[2] Shan, Y., Xiao, W., Xiang, K., Wang, B., & Zhou, S. (2022). Semi-automatic construction of pile-supported subgrade adjacent to existing railway. Automation in construction(134-Feb.).

[3] Tabrizikahou, A., & Nowotarski, P. (2021). Mitigating the energy consumption and the carbon emission in the building structures by optimization of the construction processes. Energies, 14.

[4] Wang, Y., Li, K., Zeng, X., Gao, B., & Hong, J. (2022). Energy consumption characteristics based driving conditions construction and prediction for hybrid electric buses energy management. Energy, 245.

[5] Yu, N., Chen, C., Mahkamov, K., Makhkamova, I., & Ma, J. (2021). Selection and testing of phase change materials in the physical models of buildings for heating and curing of construction elements made of precast concrete. Solar Energy, 226(1–2), 309-318.

[6] Zhang, S., Peng, K., Siqitang, W. W., & Yao, J. (2021). The matrix method of energy analysis and energy-saving design on the electromechanical system. Energy.

[7] Fan, Z., Xiao, Z., & Liu, J. P. (2022). Energy performance assessment of semi-transparent photovoltaic integrated large-scale railway stations among various climates of china. Energy Conversion and Management.

[8] Wang, J., Sekei, V. S., Ganiyu, S. A., & Makwetta, J. J. (2021). Research on the sustainability of the standard gauge railway construction project in tanzania. Sustainability, 13.

[9] Canca, D., José Luis Andrade-Pineda, De-Los-Santos, A., & Pedro Luis González-R. (2021). A quantitative approach for the long-term assessment of railway rapid transit network construction or expansion projects. European Journal of Operational Research, 294(3).

[10] Huler, M., Esser, S., & André Borrmann. (2021). Code compliance checking of railway designs by integrating bim, bpmn and dmn. Automation in Construction, 121, 103427.

[11] Qi, Q., Xu, H., Xu, G., Dong, Q., & Xin, Y. (2021). Comprehensive research on energy-saving green design scheme of crane structure based on computational intelligence. AIP Advances, 11(7), 075314.

[12] Yoshida, H. K. K. (2021). Charge/discharge control of wayside batteries via reinforcement learning for energy-conservation in electrified railway systems. Electrical engineering in Japan, 214(2).

[13] Akbari, S., Fazel, S. S., & Jadid, S. (2021). Optimal operation of a smart railway station based on a multi-energy hub structure considering environmental perspective and regenerative braking utilization. Energy Science & Engineering.

[14] Li, Z., Chen, J., & Deng, J. (2021). A feedforward air-conditioning energy management method for high-speed railway sleeper compartment. Complex Engineering Systems, 1(2), -.

[15] Jiang, L., Bie, Z., Long, T., Xie, H., & Xiao, Y. (2021). Distributed energy management of integrated electricity-thermal systems for high-speed railway traction grids and stations. CSEE journal of power and energy systems(3), 7.

[16] Thadani, H. L., Zaaba, F. D., Shahrizal, M. R. M., Arjun Singh Jaj A. Jaspal Singh Jaj, & Go, Y. I. (2021). Design and performance evaluation of vertical axis wind turbine for wind energy harvesting at railway. World Journal of Science Technology and Sustainable Development, ahead-of-print(ahead-of-print).

[17] Tomita, M., Suzuki, K., Fukumoto, Y., Ishihara, A., Akasaka, T., & Kobayashi, Y. (2017). Energy-saving railway systems based on superconducting power transmission. Energy(Mar.1), 122.

[18] Miao, R., Wu, C., Zhu, K., Xue, F., & Lu, S. (2020). Integrated optimisation model for neutral section location planning and energy-efficient train control in electrified railways. IET Renewable Power Generation, 14(10).

[19] Tong, H., Peng, J., Zhang, Y., Fang, T., & Mao, H. (2021). Environmental benefit analysis of “road-to-rail” policy in china based on a railway tunnel measurement. Journal of Cleaner Production(1), 128227.

[20] Yang, X., Liu, G., Li, Y., & Gao, S. (2021). Structural optimization of reciprocating seal with magnetic fluid based on orthogonal test design. Journal of Magnetics(2), 26.